
GAZİ ÜNİVERSİTESİ
Gazi
1926

PERFORMANCE ASSESSMENT OF REAL TIME RADAR CLASSIFICATION ON SOFTWARE-DEFINED RADIO (SDR) PLATFORMS

Seçkin ÖNCÜ

IN PARTIAL FULFILLMENT OF THE REQUIREMENTS
FOR THE DEGREE OF MASTER OF SCIENCE
IN ELECTRICAL ELECTRONIC ENGINEERING DEPARTMENT

GAZİ UNIVERSITY
GRADUATE SCHOOL OF NATURAL AND APPLIED SCIENCES

JANUARY 2024

ETHICAL STATEMENT

I hereby declare that in this thesis study I prepared in accordance with thesis writing rules of Gazi University Graduate School of Natural and Applied Sciences;

- All data, information and documents presented in this thesis have been obtained within the scope of academic rules and ethical conduct,
- All information, documents, assessments and results have been presented in accordance with scientific ethical conduct and moral rules,
- All material used in this thesis that are not original to this work have been fully cited and referenced,
- No change has been made in the data used,
- The work presented in this thesis is original,or else, I admit all loss of rights to be incurred against me.

Seçkin ÖNCÜ

08/01/2024

PERFORMANCE ASSESSMENT OF REAL TIME RADAR CLASSIFICATION ON SOFTWARE-DEFINED RADIO (SDR) PLATFORMS

(M.Sc. Thesis)

Seçkin ÖNCÜ

GAZİ UNIVERSITY

GRADUATE SCHOOL OF NATURAL AND APPLIED SCIENCES

January 2024

ABSTRACT

This thesis delves into a comprehensive analysis of the real-time classification of radar signals using software-defined radio (SDR) platforms. In the realm of electronic support measure (ESM) systems, the pulse description word (PDW) that encompasses radar signal parameters plays a pivotal role in the detection and classification of threat radars in electronic warfare (EW) scenarios. The advent of digital technologies has revolutionized radio systems, and SDR, with its software-based operations, offers unparalleled flexibility. This study presents an SDR-based radar classification system specifically designed for real-time functionality, with a strong emphasis on improved processing speed. The system employs the Density-Based Spatial Clustering of Applications with Noise (DBSCAN) algorithm as a robust classifier and harnesses the power of Graphical Processing Unit (GPU) parallelization to efficiently extract radio frequency (RF) parameters. The experimental results underscore a noteworthy enhancement in the speed of data processing as well as the precision of real-time radar classification.

Science Code	:	90523
Key Words:	:	Software defined radio, Electronic support measures, Radar classification, GPU accelaration
Page Number	:	43
Supervisor	:	Prof. Dr. Ali KARA

YAZILIM TANIMLI RADYOLAR İLE GERÇEK ZAMANLI RADAR SINIFLANDIRMA BAŞARIM ANALİZİ

(Yüksek Lisans Tezi)

Seçkin ÖNCÜ

GAZİ ÜNİVERSİTESİ

FEN BİLİMLERİ ENSTİTÜSÜ

Ocak 2024

ÖZET

Bu tez, yazılım tanımlı radyo (SDR) platformları kullanılarak gerçek zamanlı radar sınıflandırmasının kapsamlı bir değerlendirmesini sunmaktadır. Darbe tanımlama kelimesi (PDW) içinde özetlenen radar sinyali parametreleri, elektronik destek (ESM) sistemlerinde çok önemli bir rol oynayarak, elektronik harp (EW) ortamlarındaki tehdit radarlarının tespit edilmesini ve sınıflandırılmasını sağlar. Analogdan dijital teknolojilere geçiş, SDR'nin yazılım tabanlı işlemler aracılığıyla benzeri görülmemiş esneklik ve yeniden yapılandırılabilirlik sunmasıyla radyo sistemlerinde devrim yarattı. Bu çalışma, artırılmış işlem hızıyla gerçek zamanlı operasyon gerçekleştiren SDR tabanlı bir radar sınıflandırma sistemi önermektedir. Sistem, güçlü bir sınıflandırıcı olarak Yoğunluk Tabanlı Gürültülü Uygulamaların Uzamsal Kümelenmesi (DBSCAN) algoritmasını kullanır ve verimli radyo frekansı (RF) parametre çıkarımı için Grafik İşleme Birimi (GPU) paralelleştirmesinden yararlanır. Deneysel sonuçlar, gerçek zamanlı radar sınıflandırması için hem işlem hızında hem de doğrulukta önemli bir gelişme olduğunu göstermektedir.

Bilim Kodu	:	90523
Anahtar Kelimeler	:	Yazılım tanımlı radyo, Elektronik destek, Radar sınıflandırma, GPU hızlandırması
Sayfa Adedi	:	43
Danışman	:	Prof. Dr. Ali KARA

ACKNOWLEDGEMENTS

Throughout my studies, I would like to express my gratitude to my advisor, Prof. Dr. Ali KARA, for guiding me with valuable assistance and contributions, and supporting me during my graduate career. I extend my sincere thanks to my precious wife, who has always been by my side with support and prayers throughout my study, Seda Nur ÖNCÜ. I am also grateful to my colleagues, especially Rıfat DALKIRAN, Berkay SAYGILI, and Yasin AYDINLI, who motivated me and contributed to my work. I would like to express my deep appreciation to all team members. Lastly, I would like to thank TÜBİTAK BİLGEM İLTAREN for their significant contributions to the realization of this thesis.

LIST OF CONTENTS

Page

ABSTRACT iv

ÖZET v

ACKNOWLEDGEMENTS vi

LIST OF CONTENTS vii

LIST OF TABLES ix

LIST OF FIGURES x

SYMBOLS AND ABBREVIATIONS xi

1. INTRODUCTION 1

2. BACKGROUND INFORMATION 5

2.1. Radar 5

2.2. Electronic Warfare 6

2.3. Electronic Support Measures 7

2.4. Pulse Descriptor Word 7

2.5. Parallel Processing 9

2.6. Clustering 9

3. METHODS 11

3.1. Radar Classification Process 11

3.2. SDR Receiver Architecture 12

3.3. IQ Sampling Theory 14

3.4. Time Based Parameter Extraction 16

3.5. Frequency Parameter Extraction 17

3.6. GPU Acceleration 19

3.7. DBSCAN Algorithm 20

4. EXPERIMENTAL SETUP 23

Page

4.1. Radar Data Generation 23
4.2. Hardware Setup 23
4.3. Software Design 24
5. RESULTS 27
5.1. Frequency Measurement Results 27
5.2. Clustering Results 30
6. CONCLUSION 35
7. FUTURE WORK 37
REFERENCES 39
CURRICULUM VITAE 43

LIST OF TABLES

Table **Page**

Table 5.1. SDR Rx configuration for frequency measurement 27

Table 5.2. Frequency measurement test data 27

Table 5.3. Dropped packages performance of IFM and CPU/GPU FFT..... 30

Table 5.4. Clustering test setup configuration 31

Table 5.5. Threat parameters 31

LIST OF FIGURES

Figure **Page**

Figure 2.1. Subdivisions of EW 7

Figure 3.1. Radar classification process 11

Figure 3.2. Functional structure of SDR receiver 12

Figure 3.3. Block diagram of DCR architecture 13

Figure 3.4. The phasor representation of complex signal 14

Figure 3.5. IQ signal representation with I and Q signals 15

Figure 3.6. Illustration of radar pulse and some basic parameters 16

Figure 4.1. Experimental hardware configuration 24

Figure 4.2. Flowchart of proposed radar classification algorithm 26

Figure 5.1. Frequency deviation result of FFT when SNR = 20 dB 28

Figure 5.2. Frequency deviation result of FFT when SNR = 7 dB 28

Figure 5.3. Frequency deviation result of IFM when SNR = 20 dB 29

Figure 5.4. Frequency deviation result of IFM when SNR = 7 dB 29

Figure 5.5. Clusters in PW-RF plane 32

Figure 5.6. Clusters in RF-PW-PA domain 33

SYMBOLS AND ABBREVIATIONS

The symbols and abbreviations used in this study are presented below, along with their explanations.

Symbols	Explanations
MHz	Megahertz
MSps	Mega Sample Per Second
f_s	Sampling Frequency
dB	Decibel
N	Number of Samples
f_0	Center Frequency
ϵ	Epsilon
N_{min}	Minimum Points
kHz	Kilohertz
µs	Microseconds
dBm	Decibel Milliwatts

Abbreviations	Explanations
ADC	Analog to Digital Converter
AOA	Angle of Arrival
CPU	Central Process Unit
DAC	Digital to Analog Converter
DBSCAN	Density Based Spatial Clustering of Applications with Noise
DCR	Direct Conversion Receiver
DFT	Discrete Fourier Transform
DSP	Digital Signal Processing
ESM	Electronic Support Measures
EW	Electronic Warfare
FFT	Fast Fourier Transform
FFTW	Fastest Fourier Transform in the West

Abbreviations	Explanations
GPU	Graphical Processing Unit
IF	Intermediate Frequency
IFM	Instantaneous Frequency Measurement
IQ	In-phase and Quadrature
LO	Local Oscillator
PA	Pulse Amplitude
PC	Personal Computer
PDW	Pulse Descriptor Word
PRI	Pulse Repetition Interval
PW	Pulse Width
RF	Radio Frequency
RX	Receiver
SDR	Software Defined Radio
SNR	Signal to Noise Ratio
TOA	Time of Arrival
TOD	Time of Departure

1. INTRODUCTION

This section offers a synopsis of the goals of the thesis and its contributions to existing literature. Additionally, it presents a recap of the upcoming chapters and delineates the comprehensive structure of the thesis.

Motivation

One of the most important and fundamental tasks for electronic support measure (ESM) systems is the extraction of radar signal parameters. These parameters, called pulse descriptor word (PDW), which consists of radio frequency (RF), pulse width (PW), pulse amplitude (PA), time of arrival (TOA) and angle of arrival (AOA). Analyzing PDWs is important in terms of detecting and classifying the characteristic features of threat radars in electronic warfare (EW) systems [1, 2].

During the decades of the 1970s and 1980s, radio systems underwent a significant transformation as they transitioned from analog to digital technology. This shift encompassed various aspects of the systems, including system control, source and channel coding, and hardware technology. And now the software defined radio (SDR) revolution has expanded the possibilities of radio-based services by freeing them from the limitations of hard-wired characteristics such as frequency band, channel bandwidth, and channel coding. This liberation has been achieved through a combination of techniques, including the use of multi-band antennas and RF conversion, wideband Analog to Digital and Digital to Analog conversion, and the implementation of IF, baseband, and bitstream processing functions in general-purpose processors [3, 4].

SDR has recently become popular in RF signal capture solutions in the field of military and civilian applications. Technological developments and the widespread use of low-cost digital signal processors have accelerated the design of SDR. The main purpose of SDR system is to process radio signals completely digitally with a digital signal processing (DSP) unit [5]. Traditional radio systems implement modulation, demodulation, signal generation, signal processing and signal coding in the hardware part. However, SDR performs these operations in the software field. With this feature, SDR is flexible, reconfigurable and has the ability to select channels [6, 7].

The aim and contributions of this thesis

Various SDR based systems have been implemented for ESM in the literature [8-12]. In [8], an SDR based passive radar receiver platform was presented. Experimental results demonstrated that the presented system can offer 8 MHz bandwidth processing capacity to measure the position of the transmitters. In [9], the research introduces a novel approach for determining the direction of signals that is not constrained to the main lobes of antenna patterns but the division of the desired angular sector into a small number of channels, thereby achieving radar detection with reduced size, weight, costs, and computational requirements. It was shown that the sampling rate is selected as 2.4 Msps. In [10], an SDR based ESM system is proposed. The system utilizes a pulse detection algorithm with the objective of reducing the occurrence of undetected pulses caused by their overlap with other pulses, if not completely eliminating them. Experimental results showed that Fs is selected as 2.4 Msps. In [11], a scale mixture of normal distributions model is proposed to classify and cluster radar emitters. SDR is used for receiving radar signals with 4.17 Msps Fs. It can be seen that the process of clustering was solely carried out offline with the purpose of extracting information from radar signals. In [12], an SDR based radar detector was proposed. Experimental results demonstrated that the system can offer 2.4 MHz bandwidth processing capacity to classify the radars.

As can be inferred from the relevant works reported in the literature, the performance of a SDR based ESM receiver is dependent to processing speed which is directly related with sampling rate and bandwidth of SDR system [13]. Additionally, the complexity of the classification algorithm is one of the factors affecting the processing speed.

In this study, it is aimed to propose an SDR based radar classification system which work real time with higher Fs. For this purpose, a fully operational SDR based radar classification system was designed in C++ in which Density-Based Spatial Clustering of Applications with Noise (DBSCAN) algorithm is utilized as a classifier. Moreover, to speed up the process, we used Graphical Processing Unit (GPU) parallelization for RF parameter extraction. In this system, firstly, signal is received by RX port of the SDR. Then, envelope of the incoming signal is calculated. Using a threshold level, radar parameters are extracted. Next, the samples in a pulse are copied to GPU to extract RF parameter. After that, radar classification is performed by the DBSCAN algorithm, which takes PDWs as input.

The main contributions of this study can be summarized as follows:

• Sampling rate is increased up to 200 Msps for real time processing
• GPU parallelization is utilized for RF parameter extraction

Chapters of the thesis

The outline of the thesis is as follows: Chapter 2 provides information about radar, electronic warfare and radar classification. Chapter 3 presents the materials and algorithms used to develop our system. Chapter 4 describes the experimental setup. Chapter 5 presents the result of the experiments. Chapter 6 concludes the thesis with a summary of our contributions and chapter 7 shares some predictions about future work.

2. BACKGROUND INFORMATION

2.1. Radar

Radar systems, derived from the acronym of the term "RAdio Detection And Ranging," are designed to emit electromagnetic energy into a specific region of space with the aim of detecting targets within that region. The reflections from objects in the scanned space are captured by radar receivers, and through processing, information about the target, such as range, speed, and angle, is obtained. While radars were initially developed for military purposes, they have found applications beyond the military domain, including remote sensing applications, air traffic control, and various civilian uses [14].

Although originally conceived and developed for military purposes, radar systems have transcended their initial scope and have become integral components in a diverse array of applications. In addition to their military applications, radars are utilized in remote sensing practices, where they contribute to environmental monitoring and resource management. Moreover, radar systems play a crucial role in air traffic control applications, aiding in the safe and efficient navigation of aircraft. The versatility of radar technology extends to numerous civilian applications, showcasing its significance in enhancing safety, security, and efficiency across various domains [14].

Radars are classified into two main types based on the electromagnetic signal they emit into the environment: pulsed and continuous-wave radar systems. The specific tasks that radars aim to accomplish determine the signal forms and characteristics they possess. In radar systems that generate pulsed signals, characteristic features include signal frequency, pulse width, pulse repetition interval, and modulation on the pulse. On the other hand, continuous-wave radar systems exhibit characteristic features such as signal frequency and modulation of the signal. Search radars, tracking radars, and guidance radars used in military applications have distinctive characteristics in terms of their signal forms. Therefore, understanding the radar signal form is crucial, as it enables the identification of the tasks a radar intends to perform [14].

2.2. Electronic Warfare

Electronic warfare (EW) encompasses all military operations that involve the use of electromagnetic energy and diverse techniques to identify and impede hostile forces. Its primary objective is to hinder the functionality of threat radar systems while ensuring the availability of the electromagnetic spectrum for friendly forces. The implementation of electronic systems in warfare serves to protect military assets from potential enemy dangers [15].

The activities carried out within the scope of EW are categorized under three main areas: Electronic Support Measures (ESM), Electronic Counter Measures (ECM), Electronic Counter Counter Meauseres (ECCM) [15].

- ESM involves real-time threat detection and classification, providing input to the decision mechanisms of electronic attack, electronic protection, and weapon systems, while creating situational awareness.
- ECM involves rendering or deceiving enemy systems from fulfilling their functions using various techniques. Some of the techniques applied during electronic attack only temporarily disable or prevent certain functions of enemy systems, allowing them to resume normal operation once the application of these techniques ceases, without causing any permanent damage. In addition to these techniques, direct energy weapons expose enemy systems' receiver stages to high electromagnetic energy, causing them to burn, while countermeasure missiles destroy the systems. Through such methods, electronic attack renders systems completely unusable.
- ECCM aims to ensure that systems remain operational despite electronic attack techniques by implementing protective measures against them. This includes activities to secure communication lines under this domain.

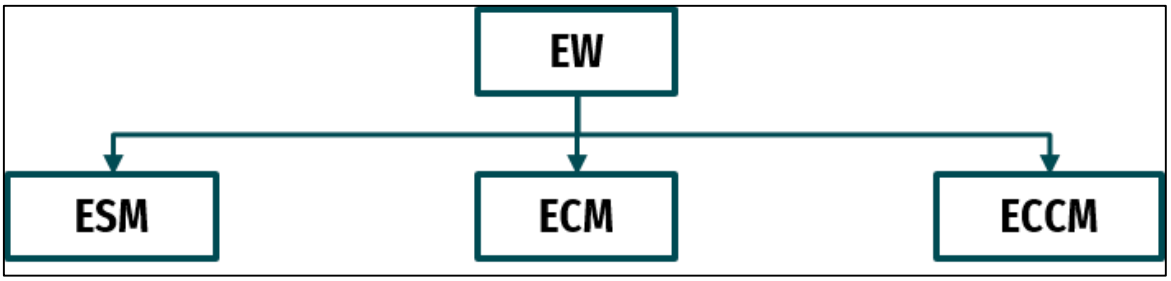


Figure 2.1. Subdivisions of EW

2.3. Electronic Support Measures

ESM is a subdomain encompassing threat detection and classification activities within EW. In the EW environment, signals from various radar systems used for purposes such as search, guidance, target tracking, and target illumination are processed in real-time by the electronic support system to acquire information about potential threats [15].

In ESM systems, the differentiation of signals in various forms based on radar types allows the identification of the threat radar type. This capability not only enables high situational awareness in ESM but also plays a critical role in determining ECM methods against the threat radar [15].

The receiver structures used in ESM systems must possess signal processing capabilities to extract distinctive parameters from passively received signals. The high frequency range of threat radars necessitates that the electronic support system operates with a broad bandwidth [15]. Particularly in threat-dense environments, the likelihood of signals arriving simultaneously at the system requires the electronic support system to process signals from multiple threats simultaneously.

2.4. Pulse Descriptor Word

The extraction and analysis of radar signal parameters play a crucial role in the identification and categorization of threat radars within ESM systems. When operating, an ESM system receives pulses transmitted by different radars in its surroundings and measures their respective parameters. These parameters primarily include the angle of arrival (AOA), radio frequency (RF), pulse width (PW), pulse amplitude (PA), and time of arrival (TOA). To

facilitate further processing, these measured pulse parameters are encoded in a digital format known as a “Pulse Descriptor Word (PDW)” [16].

Pulse Width (PW): The duration between the rising edge and falling edge of the pulse envelope is referred to as PW. This particular parameter provides valuable insights into the type of threat radar being used. For instance, weapon systems integrated with radars typically employ short pulses. The duration of these pulses can vary from tens of nanoseconds to hundreds of microseconds [16].

Pulse Amplitude (PA): The average amplitude value derived from the pulse envelopes. Utilizing the PA parameter enables the identification of the search pattern employed by the threat radar. It also provides information about the distance of the radar, but the accuracy of the range information estimated by PA is not very high [16].

Time of Arrival (TOA): The moment when the pulse reaches the radar receiver. On the other hand, the Pulse Repetition Interval (PRI) parameter is determined by calculating the time difference between the start or end times of two consecutive pulses [16].

Radio Frequency (RF): It is the frequency information carried by the radar pulse. Radar systems typically operate within a frequency range spanning from 200 MHz to 95 GHz. Nevertheless, certain radar systems have the capability to operate at frequencies below 2 MHz and above 300 GHz. However, the most commonly used frequency band is the 2 GHz-18 GHz band. It is crucial to ascertain the frequency parameter of radars operating within this band range for the purposes of pulse separation, as well as the implementation of jamming and deception techniques. Once the frequency and identity of the radar posing a threat are determined, the jammer focuses all its energy on the relevant frequency band, thereby establishing an effective ECM [16].

Angle of Arrival (AOA): This parameter plays a crucial role in determining the radar's position. Given the difficulty for the threat radar to constantly alter its location, AOA becomes a reliable parameter for threat detection. This parameter can be analyzed in two distinct categories: elevation and azimuth plane. However, calculating AOA is a complex task [16].

2.5. Parallel Processing

Parallel computing is a concept that aims to distribute the workload across multiple resources in order to enhance computational speed. In order to effectively perform tasks in parallel, several factors need to be considered, including the independence of tasks and the requirement for sequential execution. Certain algorithms pose inherent challenges when it comes to parallel execution, while others exhibit favorable scalability with an increase in the number of threads utilized. Over the past decade, multi-core chips have played a significant role in powering various applications, and the utilization of GPUs has witnessed a notable surge. GPUs are equipped with a substantial number of cores and offer an economical alternative to the development of specialized hardware like Field-Programmable Gate Arrays (FPGA) [17].

2.6. Clustering

Clustering refers to a technique that involves grouping the parameters that describe an object in such a way that the objects within a group exhibit stronger relationships with each other compared to objects in separate groups. There exists a wide range of clustering methodologies that can be utilized to categorize data of varying sizes based on diverse metrics. These methodologies and algorithms possess distinct characteristics that render them suitable for different types of data, contingent upon the inherent structures within the data and the assumptions that can be made regarding its distribution. Clustering methods rely on the similarities and dissimilarities of stationary emitter parameters such as PF, PW, and AOA. In certain specific situations, PA may also be applicable [18].

3. METHODS

3.1. Radar Classification Process

The primary purpose of an ESM system is to detect threats and conduct surveillance of a specific area in order to identify the sources of electromagnetic emissions. This system is designed to analyze the pulse-by-pulse measurements obtained by the receiver, enabling it to identify known radars and indicate their presence [19, 20]. Figure 3.1, shows the basic stages of ESM. [19, 20]. As depicted in Figure 3.1, the receptor part of the system consists of an antenna that captures RF signals and transmits them to the ESM receiver. The received signal is then digitized and forwarded to the processor. The processor analyzes the pulse parameters, and the identified pulses are converted into PDWs, which include parameters such as TOA, PW, RF and PA. As a result of this process, the PDW is sent to the deinterleaving and clustering stage. The deinterleaved signal is then directed to the classifier, which compares it with the emitter database. If the measured parameters of a threat signal align with one of the parameter sets in the database, it is concluded that the corresponding threat is present. Conversely, if the collected parameters do not match any parameter sets in the database, the signal is classified as unknown. Finally, the classification results are presented to the users on a display, which can be viewed either in tabular or graphical format, facilitating easy interpretation and comprehension of the data [21-23].

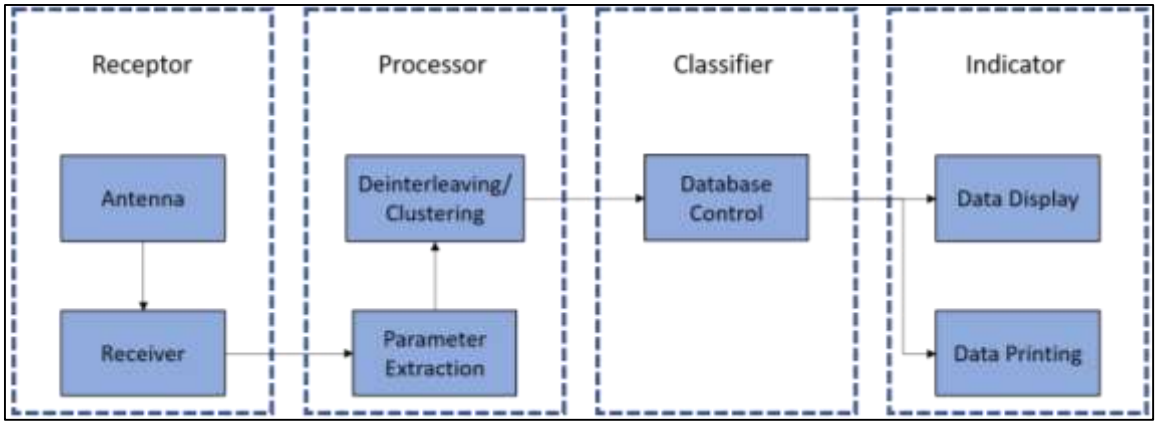


Figure 3.1. Radar classification process

3.2. SDR Receiver Architecture

In conventional radios, dedicated components are responsible for carrying out specific functions, including modulating/demodulating signals, encoding/decoding data, and more. These specialized hardware components handle all aspects of signal processing. However, software defined radio technology introduces a paradigm shift by replacing certain traditional radio components with software-based implementations. The ability to program or configure the hardware through software provides further flexibility and customization options in SDR architecture. [24].

The SDR receiver can be divided into two primary components: the analog front-end and the DSP components. The analog front-end is responsible for the narrowband frequency down conversion and the subsequent analog-to-digital conversion (ADC). On the other hand, the digital signal processing components handle the remaining signal processing tasks such as demodulation, filtering, and channel decoding. These operations are carried out in the digital domain. The data flow in a software-defined radio receiver system is depicted in Figure, illustrating that the majority of baseband signal processing is performed using software. The functional structure of an SDR receiver system is depicted in Figure 3.2. The RF front-end downconverts the intercepted analog signal to a baseband frequency, enabling it to be sampled and processed by an ADC. The digital IF signal that ensues is subsequently directed towards the DSP components, where it undergoes additional processing such as demodulation, filtering, and channel decoding. The software-based approach is widely employed in baseband signal processing, enabling the SDR receiver architecture to possess remarkable flexibility and adaptability [25-27].

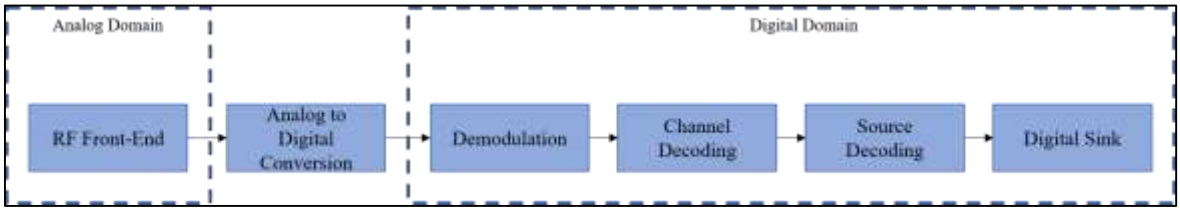


Figure 3.2. Functional structure of SDR receiver

SDR Architecture possesses several significant benefits. SDR systems exhibit flexibility by allowing the receiver's functionality to be altered through software, thereby facilitating dynamic reconfiguration and adaptation to diverse signal types and communication

protocols. Moreover, SDR systems have the potential to decrease hardware expenses by substituting dedicated hardware components with software-based implementations. Additionally, SDR systems can be effortlessly scaled to meet varying bandwidth requirements and processing demands. Lastly, SDR systems can adhere to open standards, thereby fostering interoperability and compatibility with a wide range of software and hardware components [26, 27].

In the realm of RF front-end stage, the direct conversion receiver (DCR) architecture is widely utilized in SDR. DCRs have become increasingly popular due to their inherent superiority over superheterodyne receivers. The distinguishing feature of the DCR architecture lies in its compactness, as it achieves frequency translation from RF to baseband in a solitary mixing stage. This direct down-conversion approach enables signal amplification and filtering at baseband, resulting in decreased power consumption and simplified image rejection. These combined advantages play a pivotal role in implementing the entire receiver as a monolithic integrated circuit, thereby reducing manufacturing costs [28-30].

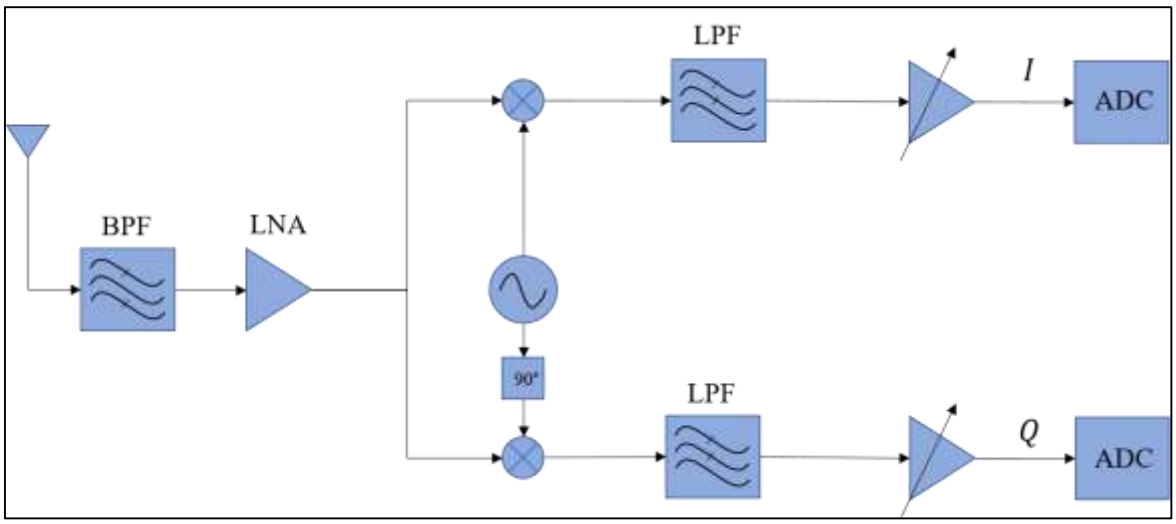


Figure 3.3. Block diagram of DCR architecture

Block diagram of a DCR architecture is depicted in Figure 3.3. Firstly, the incoming RF signal is subjected to filtration and amplification in order to guarantee the optimal signal quality. Following this, the process of downconversion to baseband is achieved by utilizing a pair of mixers and the quadrature sinusoids that combine to form the complex sinusoid. This resulting complex signal is then subjected to filtration through two lowpass filters, one

in I-channel (in-phase) and the other in the Q-channel (quadrature). The ADC then transforms the analog IF signal into a digital representation, facilitating subsequent processing in the digital domain. [28-30].

3.3. IQ Sampling Theory

IQ sampling, also referred to as quadrature sampling, is the sampling technique employed by software-defined radios (SDRs), as well as numerous digital receivers and transmitters. The acronym "IQ" represents in-phase (I) and quadrature-phase (Q), which are two orthogonal components that collectively represent a complex signal. I and Q components are mathematical constructs that enable the representation of a signal in a two-dimensional space. The phasor form in the Figure 3.4, illustrates the I and Q components of a signal. IQ sampling is utilized to capture the amplitude and phase of a carrier signal that has been modulated to transmit data or information. The I component signifies the amplitude of the cosine wave (real part), while the Q component represents the amplitude of the sine wave (imaginary part). IQ sampling offers several advantages, including the ability to represent negative frequencies, which is crucial for numerous signal processing techniques. Additionally, it allows for more efficient utilization of bandwidth [31].

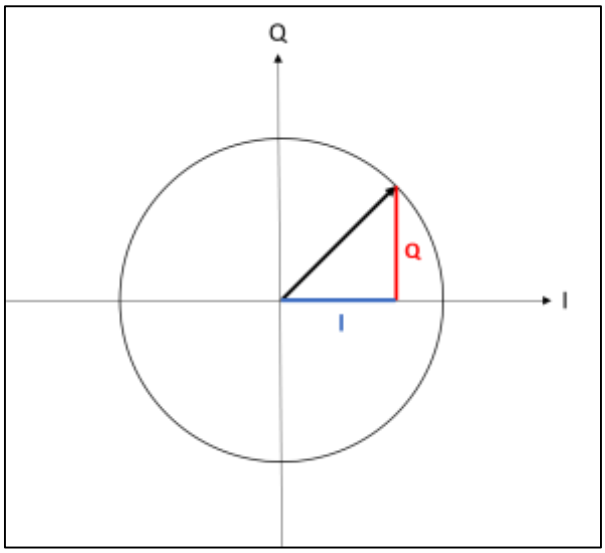


Figure 3.4. The phasor representation of complex signal

The IQ signal is considered a complex signal because it combines the I and Q components, resulting in a complex number at each sampling point. The complex IQ signal is obtained by adding the I signal and the Q signal. By adjusting the amplitude values of the I and Q signals,

the overall amplitude and characteristics of the complex IQ signal can be modified, as depicted in the Figure 3.5.

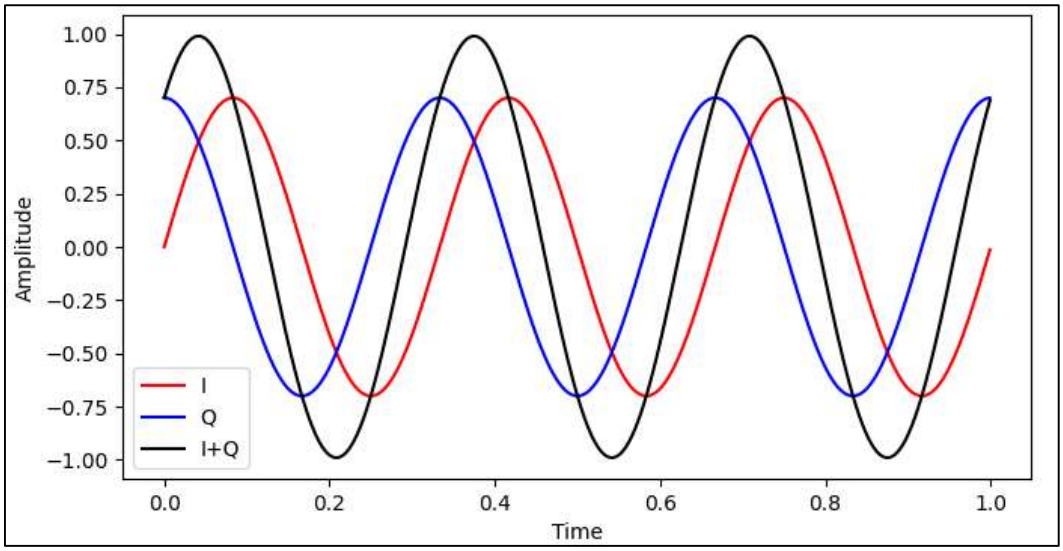


Figure 3.5. IQ signal representation with I and Q signals

Mathematically, a real bandpass signal can be expressed as [32]

$$x(t) = r(t)\cos(2\pi f_0 t + \phi_x(t)) \tag{3.1}$$

where $r(t)$ represents the envelope of a bandpass signal, $\phi_x(t)$ denotes the time-varying phase of the signal. The carrier frequency is denoted as f_0. It is important to highlight that both $r(t)$ and $\phi_x(t)$ exhibit frequency components considerably smaller than f_0.

The representation of bandpass signals can be equivalently expressed through the utilization of two lowpass signals, commonly referred to as quadrature components, within the framework of the complex envelope representation. This is elucidated as follows

$$x(t) = x_I(t)cos2\pi f_0 t - x_Q(t)sin2\pi f_0 t \tag{3.2}$$

where $x_I(t)$ and $x_Q(t)$ are real lowpass signals referred to as the quadrature components and are given by

$$x_I(t) = r(t)\cos\phi_x(t) \tag{3.3}$$

$$x_Q(t) = r(t)\sin\phi_x(t) \tag{3.4}$$

3.4. Time Based Parameter Extraction

The envelope detector unit is essential for the extraction of all parameters in the parameter extraction block. The signal in IQ format, entering the parameter extraction block, is first directed to the envelope detector block. Through this block, time parameters of the pulse signal, such as TOA, PW, PA, are determined. Simultaneously, the envelope information of the pulse, which will be utilized in extracting RF parameter, is also obtained through the envelope detector block. [33]. The parameters of radar pulse are illustrated in Figure 3.6.

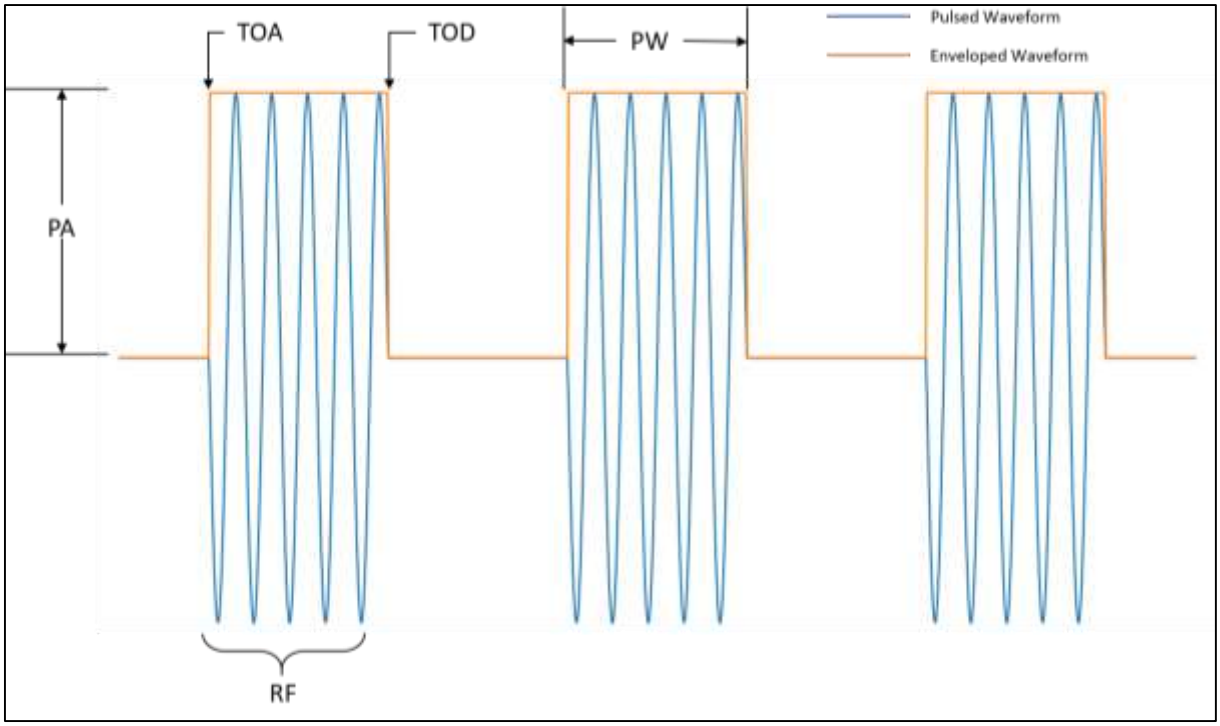


Figure 3.6. Illustration of radar pulse and some basic parameters

As can be referred from Eq.3.1, Eq.3.3 and Eq.3.4, the envelope of IQ signal can be expressed as

$$r(t) = \sqrt{x_I(t)^2 + x_Q(t)^2} \tag{3.5}$$

After the extraction of the signal envelope, the process transitions to the detection of whether there is a threat signal in the environment. If the envelope of the signal surpasses the

threshold value determined by the noise level, it is understood that there is a threat in the environment, and the parameter extraction process is initiated.

In instances where the current amplitude of the sample surpasses the predetermined threshold, while the amplitude of the preceding sample falls below the threshold level, the count of that particular sample is retained as the TOA in sample count. Hence, the division of this value by the sample rate yields the TOA.

In instances where the current amplitude of a sample falls below the threshold while the preceding sample amplitude surpasses the threshold, the current sample number provides the time of departure (TOD) in sample count. Hence, the division of this value by the Fs yields the TOD. PW is obtained by difference of TOD and TOA.

$$PW = TOD - TOA \tag{3.6}$$

In the proposed design, pulse amplitude (PA) can be obtained by

$$PA = \sum_{i=0}^{N} \frac{r_i(t)}{N} \tag{3.7}$$

where N represents the total number of samples in the pulse and $r_i(t)$ represents each individual sample in the pulse.

3.5. Frequency Parameter Extraction

In this thesis, real-time extraction of the frequency parameter has been implemented using two different methods, namely Instantaneous Frequency Measurement (IFM) and Fast Fourier Transform (FFT). Mutual analyses in real-time applications have been conducted under various conditions. The working principles of these methods will be theoretically explained in this section.

FFT is a computational algorithm utilized for the computation of the discrete fourier transform (DFT) of a sequence. The DFT is a mathematical transformation that uncovers the frequency components of a signal or a set of data. DFT has finite length N and pairs for finite sequence $x(n)$ are defined as follows [32]

$$X(k) = \sum_{n=0}^{N-1} x(n) e^{-\frac{j2\pi nk}{N}} \quad ; k = 0, \dots, N-1 \tag{3.8}$$

When a given N-point FFT is employed, the input frequency band is divided into N, f_s/N filters. Consequently, the FFT operation is executed on each incoming sample in the pulse. After FFT implementation, which FFT bin has the peak magnitude can be found. To obtain the index which has maximum frequency

$$k_{max} = argmax_k |X(k)| \tag{3.9}$$

and the shift in the frequency can be found as follows

$$f_{max} = \frac{k_{max} * f_s}{N} \tag{3.10}$$

So, RF parameter can be found as

$$RF = f_0 + f_{max} \tag{3.11}$$

The technique of Instantaneous Frequency Measurement (IFM) is utilized for the estimation of frequencies of multiple simultaneous signals. This approach involves analyzing the autocorrelation of the received signals to determine their individual frequencies. By utilizing the available I and Q samples, the phase can be determined using the provided equation. [32]

$$\phi_x(t) = \tan^{-1} \frac{x_Q(t)}{x_I(t)} \tag{3.12}$$

In the next, frequency modulation can be found as

$$\mathrm{f}_m(t) = \frac{1}{2\pi} \frac{d}{dt} \phi_x(t) \tag{3.13}$$

So, RF parameter can be found as

$$RF = f_0 + f_m(t) \tag{3.14}$$

FFT and IFM are two signal processing techniques that have different applications and operate in distinct manners. FFT is a powerful tool for examining the frequency makeup of

a signal as it evolves, allowing for a deeper understanding of its frequency properties. On the other hand, IFM concentrates on swiftly identifying the immediate frequency of a signal, providing up-to-the-minute details about its frequency fluctuations. The selection between FFT and IFM hinges on the unique characteristics of the signal in question and the desired information. Although IFM provides uninterrupted frequency tracking, its precision is susceptible to the presence of noise. Furthermore, the outcomes of FFT are impacted by the specific frequency components that exist within the signal being analyzed. [34].

3.6. GPU Acceleration

Performing frequency measurement using FFT can be computationally demanding, especially when dealing with large datasets. Executing the FFT process in parallel via the Graphics Processing Unit (GPU) allowed us to free up the Central Processing Unit (CPU) memory and to perform other important calculations faster on CPU. The proposed parallel implementation aims to offload the most time-consuming tasks to the GPU, thereby enhancing overall performance. Furthermore, optimizing memory allocation and minimizing input/output transfers between the CPU and GPU are essential for efficient execution [35, 36].

The Nvidia CUDA Fast Fourier Transform library (cuFFT) offers a streamlined interface for efficiently computing FFTs on GPUs, eliminating the need to create a customized GPU FFT implementation [37]. To facilitate the computation of FFTs on an NVIDIA GPU, the cuFFT library offers a straightforward interface. This library enables users to promptly harness the immense floating-point capabilities and parallelism of the GPU, while benefiting from a highly optimized and thoroughly tested FFT library [38-40].

The cuFFT algorithm is designed based on FFTW [41], a widely used and highly efficient CPU-based FFT library. The cuFFT algorithm offers a straightforward plan configuration mechanism that utilizes internal components to optimize the transform for the specific configuration and GPU hardware chosen. For our study, we used 1D DFT which has forward and backward computations. Forward DFT computation stores the positive frequencies in the first half of the output. However, backward DFT computation stores the negative frequencies in the first half of the output. Subsequently, the subsequent backward DFT

converts a representation in the frequency domain back to the initial signal in the time domain.

$$X(k) = \sum_{n=0}^{N-1} x(n) e^{\frac{j2\pi nk}{N}} \quad ; k = 0, \dots, N-1 \tag{3.15}$$

3.7. DBSCAN Algorithm

Radar pulse clustering plays a vital role in extracting significant insights from radar signals. Within the realm of clustering algorithms, Density-based spatial clustering of applications with noise (DBSCAN) stands out as a highly effective method for handling noise, outliers, and diverse densities within the data. Unlike conventional clustering algorithms that rely on predetermined cluster shapes or centroids, DBSCAN identifies clusters based on the local density of data points, enabling it to effectively handle noise and variations in cluster shapes. Furthermore, DBSCAN's capability to identify clusters of arbitrary shapes and sizes makes it particularly well-suited for analyzing radar pulse data, which often exhibits non-uniform densities and shapes [42-44].

This algorithm performs clustering by calculating the distances of objects from their neighbors and grouping areas with more objects than a predetermined threshold value in a certain region. The algorithm takes epsilon (ϵ) and minimum points (N_{min}) values as input parameters. It checks all objects, starting from any object in the database. If the controlled object has already been included in a set, it moves to the other object without taking action. If the object has not been clustered before, it finds the object's neighbors in the ϵ neighborhood by making a region query [42]. Drawing upon the principles outlined in [42, 45], we implemented the DBSCAN algorithm in our work.

The ϵ- neighborhood of a point x can be defined as

$$N_\epsilon(x) = \{y \in D : d(x, y) \leq \epsilon\} \tag{3.15}$$

where D is the data set and $d(.,.)$ is a certain distance function.

If the number of neighbors exceeds N_{min}, the current data point and its neighbors are designated as a new cluster. Subsequently, new neighbors are identified for each unclustered neighbor within the epsilon neighborhood.

A point x is said to be directly density reachable from a point y (with respect to ϵ and N_{min}) if for $x \in N_\epsilon(y)$, $|N_\epsilon(y)| \geq N_{min}$ where $|N_\epsilon(y)|$ denotes the number of points in $N_\epsilon(y)$.

Data points within the epsilon neighborhood of the region query point are deemed part of the cluster if their number exceeds N_{min}, forming a density-connected region. Two points, x and y, are considered density-connected with respect to ε and N_{min} if there exists a point, z, such that both x and y are density-reachable from z with respect to ε and N_{min}. This implies that a chain of density-reachable points connects x and y, with each point having at least minPts neighbors within the epsilon neighborhood [45].

Data points located within the epsilon vicinity of the region query point are classified as members of the cluster if their count surpasses N_{min}, thereby constituting a density-connected region. In the context of ϵ and N_{min}, two points, x and y, are regarded as density-connected if there exists a point, z, such that both x and y are density-reachable from z with respect to ϵ and N_{min}. This condition implies that a sequence of density-reachable points connects x and y, where each point possesses at least minPts neighbors within the epsilon neighborhood.

Let D be a data set. A cluster C with respect to ϵ and N_{min} is a nonempty subset of D satisfying the following conditions

- $\forall x, y \in D$, if $x \in C$ and y is density-reachable from x with respect to ϵ and N_{min}, then $y \in C$
- $\forall x, y \in C$, if x and y is density-connected with respect to ϵ and N_{min}

The identification and differentiation of radar sources can be effectively achieved by utilizing several parameters for radar signal clustering. Among these parameters, AOA, RF and PW are the most reliable parameters for the radar clustering [46, 47]. Unfortunately, our single-channel system has certain limitations that prevent us from extracting AOA information. As a result, we had to utilize the DBSCAN algorithm in our research to cluster

PDW data, with RF and PW parameters serving as the main features. By adopting this approach, we were able to effectively utilize the provided information and group radar signals based on their RF and PW characteristics. Consequently, we could successfully identify and differentiate various radar sources.

4. EXPERIMENTAL SETUP

4.1. Radar Data Generation

A sophisticated commercial environment simulator is utilized to generate the radar signals, serving as a vital tool for testing and evaluating advanced electronic warfare (EW) and radar receiver systems. This comprehensive simulator is capable of producing realistic simulations that emulate various radar environments with multiple threats. Its main objective is to test and evaluate EW systems by generating real-time RF signals with preprogrammed threat characteristics. These simulations take place in a controlled and simulated environment, guaranteeing accuracy and reproducibility in the experimental setup. In addition to conventional radars, the simulator is capable of accommodating frequency hopping and frequency agile radars. It also supports pulse to pulse and group to group frequency changes. To replicate the impact of measurement noise, a Gaussian noise with a specified variance is introduced to the frequency. The simulator also provides support for radars that can change pulse width. As pulse width measurements are susceptible to being influenced by the power amplifier level, a Gaussian noise is incorporated into the pulse width to replicate these measurement inaccuracies. The simulator produces pulses from each radar separately and subsequently combines them in chronological order by merging the pulses associated with all radars and arranging them based on their TOA. Additionally, the simulator accounts for the impact of overlapping pulses in time.

4.2. Hardware Setup

Figure 4.1, depicts the experimental setup employed for real-time classification of radar signals utilizing SDR technology. The radar signals are generated using a commercial environment simulator and RF combiner is used to merge the RF signals emanating from various ports of the environment simulator.

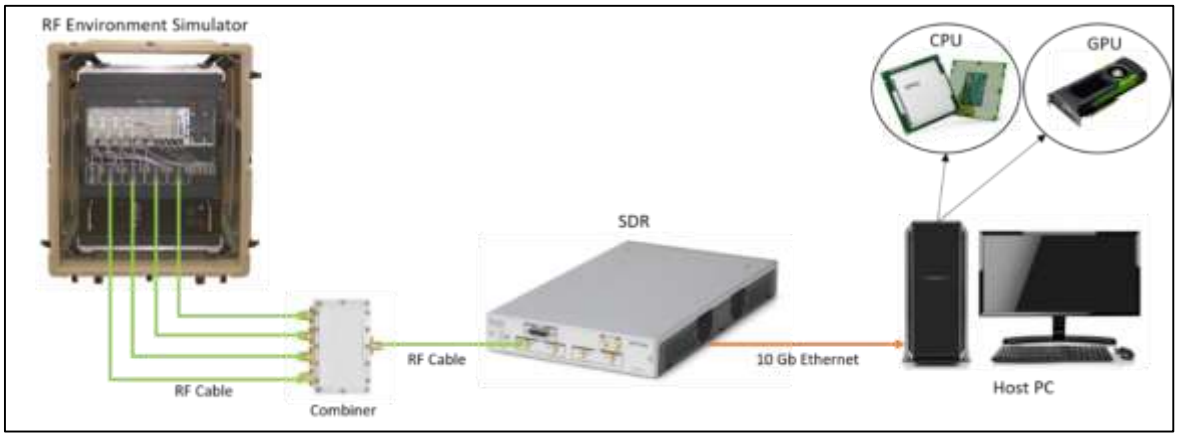


Figure 4.1. Experimental hardware configuration

The SDR receives RF signals through its Rx port and is connected to the combiner via an RF cable. Once connected, the SDR digitizes the received RF signal and converts it into IQ data. This IQ data is then transmitted to the host PC using a dual 10-gigabit Ethernet interface for further analysis and real-time classification. This hardware configuration, utilizing the capabilities of SDR technology and an RF Environment Simulator, provides a reliable platform for evaluating and classifying radar signals in controlled scenarios. For this purpose, the Ettus USRP N320 SDR [48] is utilized, which offers a frequency range of 3 MHz to 6 GHz and an instantaneous bandwidth of 200 MHz per channel.

4.3. Software Design

The iterative structure within an infinite loop is employed for the main code implementation. The primary goal is to extract pulsed radar parameters using a multi-step procedure as described in earlier sections. Initially, the signal is subjected to envelope extraction in order to distinguish pulse characteristics. Once the pulses are identified, the corresponding samples are sent to the GPU for FFT computation, utilizing the cuFFT algorithm. The resulting pulse parameters are methodically recorded in a PDW array. When the number of entries in the PDW array reaches 100, the DBSCAN algorithm is invoked to identify distinct clusters within the radar signals. Simultaneously, the PDW array is reset to eliminate previous data, and the associated counters are reset to ensure the ongoing integrity of the data.

The intricate steps of the radar classification algorithm are depicted in the Figure 4.2, providing a comprehensive visual representation of the parameter extraction and clustering procedure. This iterative and parallelized approach guarantees the efficient extraction and analysis of relevant radar signal information, thereby facilitating subsequent stages of data interpretation and decision-making within the radar processing framework.

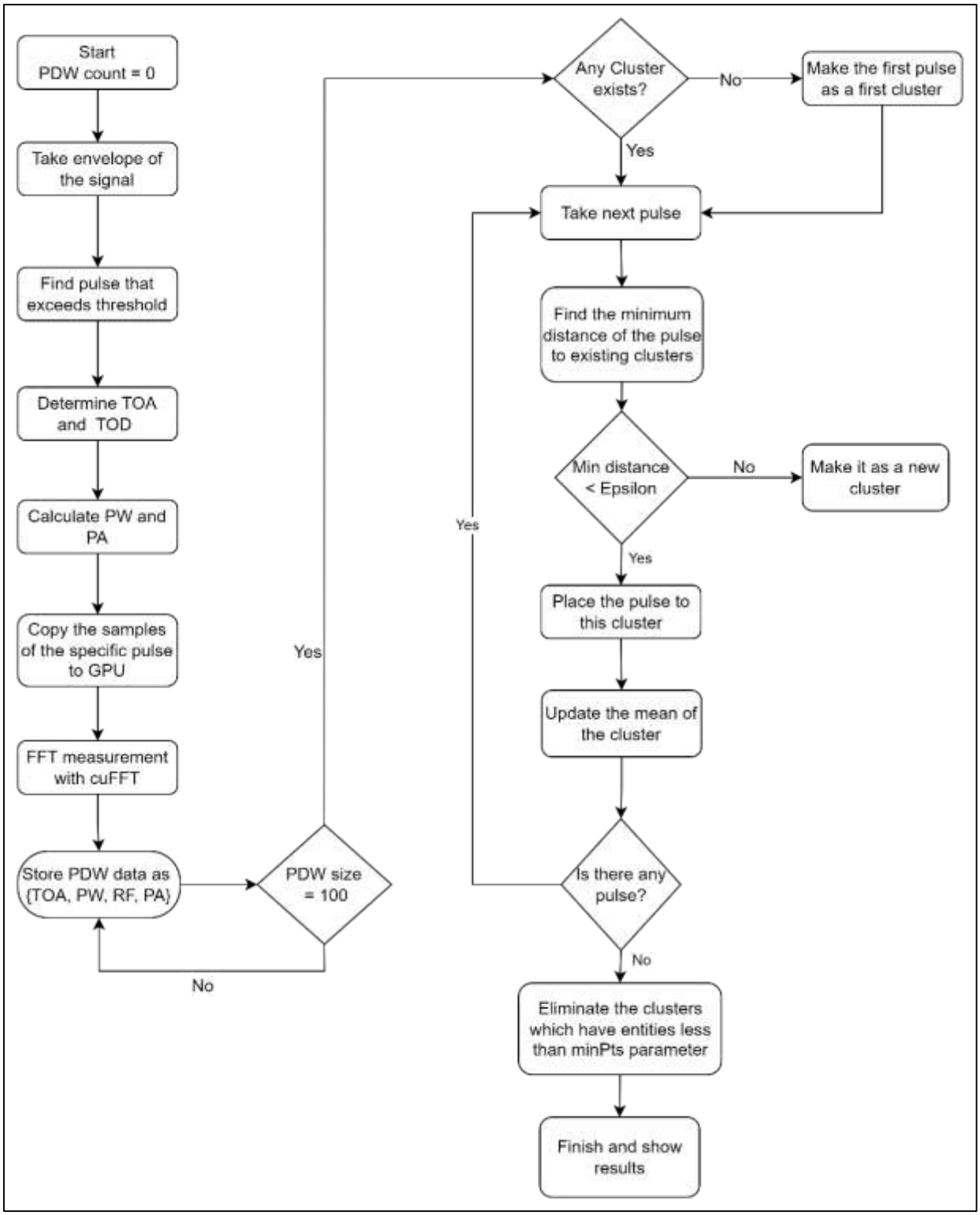


Figure 4.2. Flowchart of proposed radar classification algorithm

5. RESULTS

5.1. Frequency Measurement Results

In the preceding sections, we have discussed the utilization of both the FFT and IFM techniques for frequency estimation. The Table 5.1 and Table 5.2 and provided below present the parameters of the SDR receiver and the test data that was generated, respectively. To generate the test data, the RF environment simulator was employed, and subsequently, the SDR processed it. Within the SDR framework, a comparative analysis was conducted by performing FFT computations on both the CPU and GPU platforms, along with IFM computation solely on the CPU.

Table 5.1. SDR Rx configuration for frequency measurement

Sampling rate	10 MSps
Center Frequency	1502.5 MHz
FFT size	1024

Table 5.2. Frequency measurement test data

Number of Pulses	50
Frequency	1500 – 1505 MHz, 100 kHz steps
PW	10 μs
Duty Cycle	10 %
SNR	20 dB, 7 dB

Some of the results regarding with the frequency deviation in kHz are presented in Figure 5.1, Figure 5.2, Figure 5.3 and Figure 5.4.

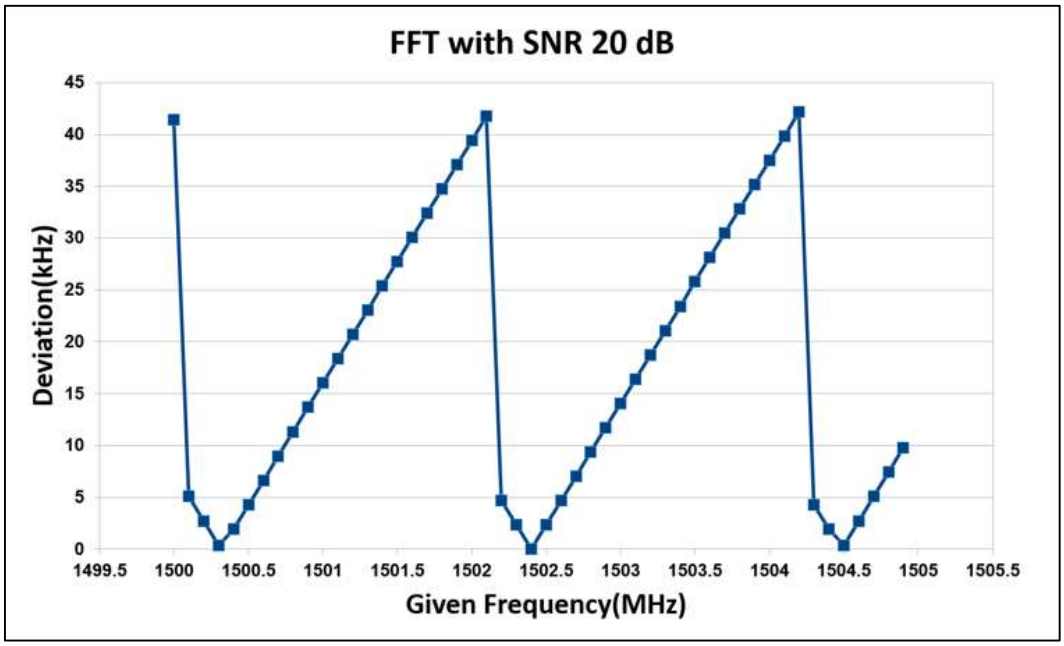


Figure 5.1. Frequency deviation result of FFT when SNR = 20 dB

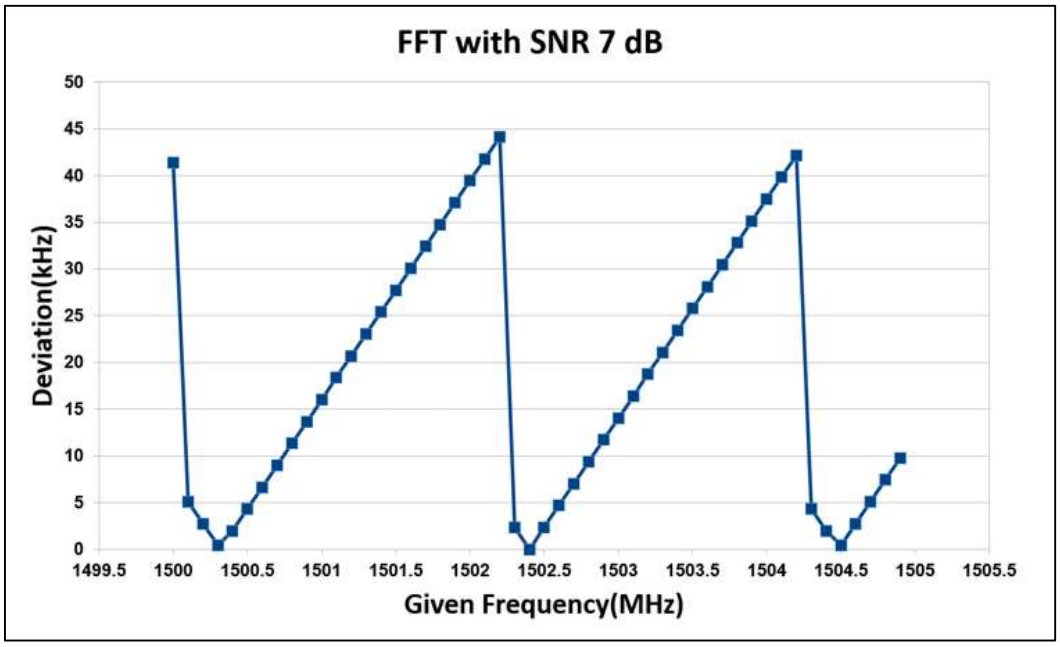


Figure 5.2. Frequency deviation result of FFT when SNR = 7 dB

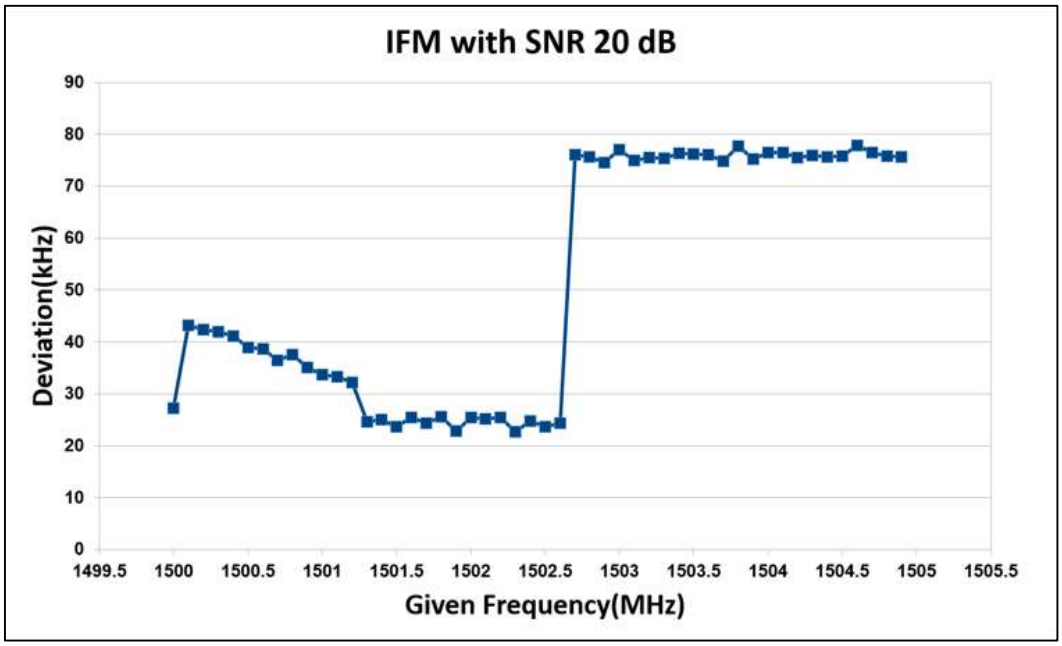


Figure 5.3. Frequency deviation result of IFM when SNR = 20 dB

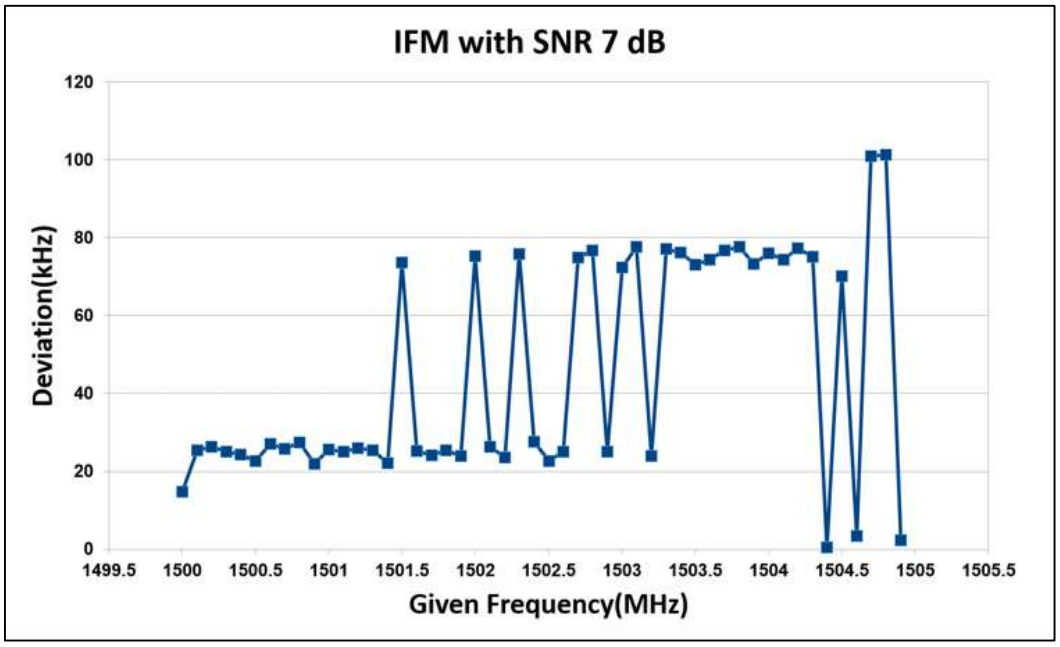


Figure 5.4. Frequency deviation result of IFM when SNR = 7 dB

The presented figures demonstrate a comparative analysis of the data, revealing a higher level of accuracy in the results obtained through the FFT in contrast to those derived from the IFM. It is particularly noteworthy that the FFT algorithm exhibits robustness in the presence of signal noise, yielding outcomes that align with the expected results. This resilience can be attributed to the inherent correspondence between the FFT bins and the frequency components of the signal, which enhances the algorithm's ability to mitigate the

impact of noise and provide reliable spectral information. Chapter 3.5 further supports this observation, indicating that the FFT algorithm displays greater resilience when faced with low SNR values.

Additionally, we conducted a comparison of the algorithms' processing speed. To assess this, we implemented various sampling rates and continuously applied an RF signal with the same parameters as outlined in Table 5.2. Consequently, we observed a drop in packages received by the SDR when the signal was received. As the rate of package dropout increased, there was a corresponding escalation in processing time. The detailed results of this analysis can be found in Table 5.3.

Table 5.3. Dropped packages performance of IFM and CPU/GPU FFT

Sampling Rate	IFM	FFT(N=1024) on CPU	FFT(N=1024) on GPU
50 MSps	0	0	0
100 MSps	0	10	0
200 MSps	20	50	0

As a result of this experiment, we opted for FFT due to its greater robustness. While it exhibits slower CPU performance compared to IFM, we chose to implement FFT on a GPU using the cuFFT algorithm. With this approach, no sample dropping errors were observed at peak capacity.

5.2. Clustering Results

The evaluation of the proposed system using the acquired dataset is discussed in this section. The testing configurations can be found in Table 5.3. The threat parameters, which are assumed to exist in the environment, are listed in Table 5.5. In addition, Gaussian-distributed errors were introduced to the RF parameters. The operational sequence of each radar depended on the emission of a predetermined number of pulses by its predecessor. The culmination of this sequential radar operation is visually represented in a two-dimensional diagram that illustrates the relationship between RF and PW parameters, as explained in previous sections. This diagram, shown in Figure 5.5 and Figure 5.6 captures the emergent patterns and associations within the radar data, providing a comprehensive depiction of the interplay between RF and PW parameters across the radar network. The identified radar

signals are as follows: Radar 1 is identified as Threat 3, Radar 2 as Threat 4, Radar 3 as Threat 5, Radar 4 as Threat 6, Radar 5 as Threat 2, Radar 6 as Threat 7, Radar 7 as Threat 8, and Radar 8 as Threat 1.

Table 5.4. Clustering test setup configuration

Sampling rate	200 MSps
Center Frequency	4013 MHz
FFT tap size	1024
Distance (ϵ)	1
Data points ($N_{\min)}$	5

Table 5.5. Threat parameters

Radar No.	RF (MHz)	PW (µs)	PRI (µs)	PRI Type	PA (dBm)	#Pulses
1	4000	0.4	113-317-419	Staggered	-17	19
2	4003	0.6	89-199	Dwell-Switch (9 pulses)	-20.1	18
3	4006	0.8	211	Constant	-23	10
4	4009	1	271	Constant (±%3 jittered)	-25	10
5	4012	2	547	Constant	-22	10
6	4015	0.5	73-101-103	Staggered	-22	20
7	4020	0.75	337-457	Dwell-Switch (5 pulses)	-19	20
8	4025	0.9	991	Constant	-18	20

As a result of the outlined scenario, a PDW array was utilized to extract and systematically store a total of 1000 pulses. Following the clustering stage, it was determined that 929 pulses were successfully allocated to distinct clusters. The visual representations presented in the figures confirm the precise clustering of all 8 distinct radars, highlighting the effectiveness of the clustering methodology.

Upon closer examination of the clusters, a detailed observation revealed that 32 pulses were mistakenly assigned to clusters. However, the overall accuracy of the clustering process

remained commendable, as 897 pulses out of the initial 1000 were accurately assigned to their respective clusters. This demonstrates the strong performance of the clustering algorithm in effectively categorizing the majority of pulses, thus validating its efficacy in the context of radar signal processing..

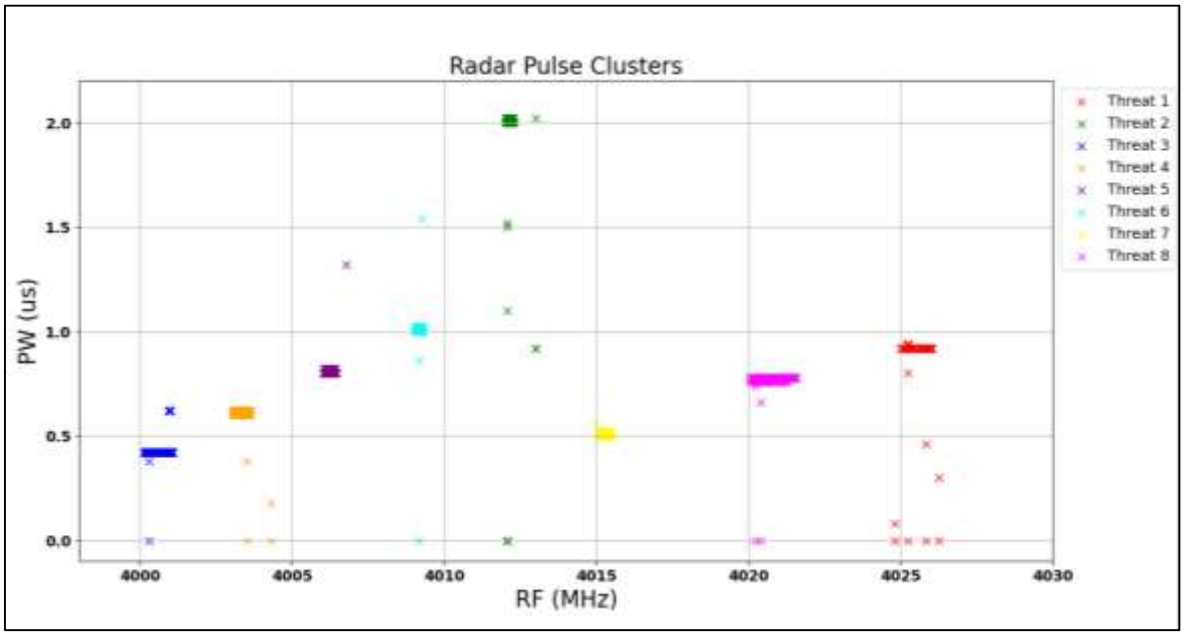


Figure 5.5. Clusters in PW-RF plane

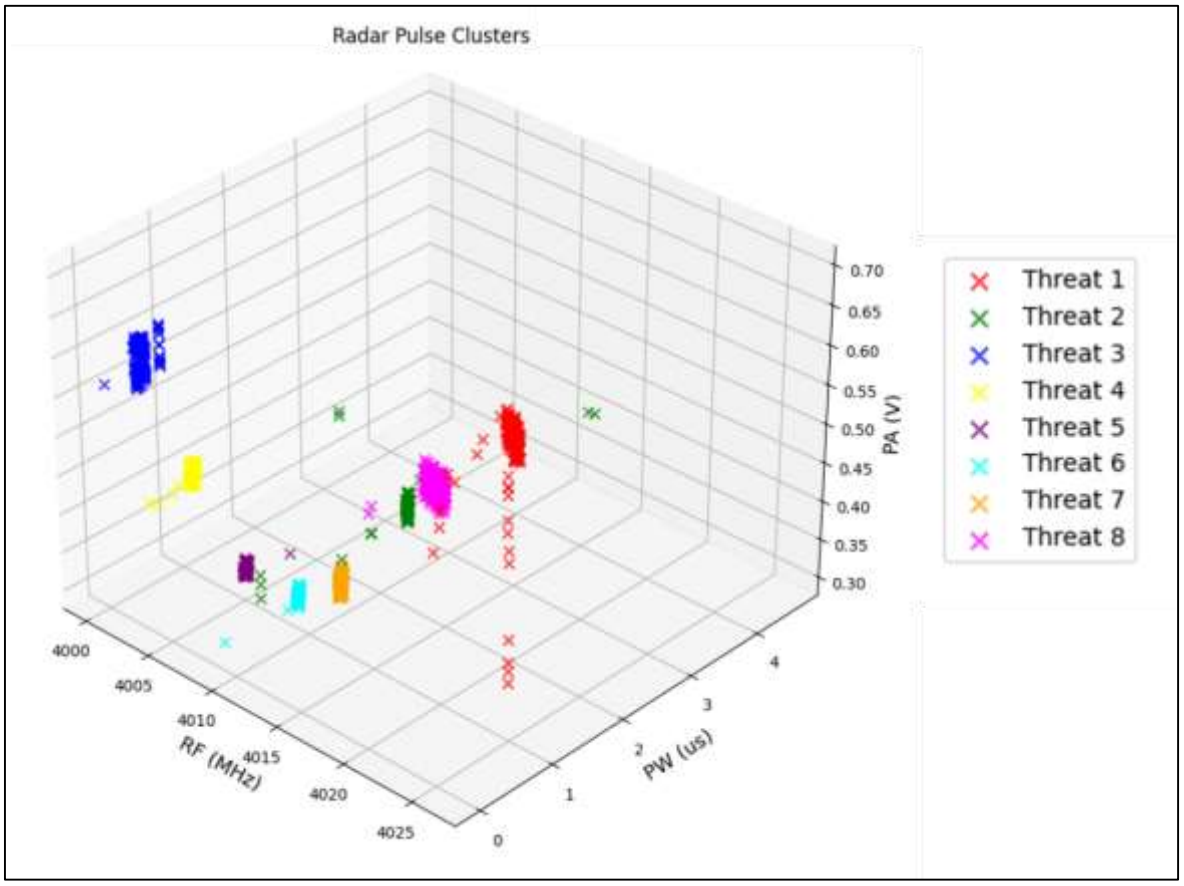


Figure 5.6. Clusters in RF-PW-PA domain

6. CONCLUSION

Throughout this study, we have successfully developed and implemented a real-time radar classification system based on SDR. The thesis extensively covers the intricate design and operational details of this system. Additionally, a comprehensive performance evaluation has been conducted to thoroughly assess its effectiveness and capabilities in classifying real-time radar signals. A strategic decision was made to offload resource-intensive FFT computations to the GPU for parallel frequency parameter estimation. This approach has proven to be highly effective, as it optimizes resource utilization and reduces the computational burden on the CPU. Consequently, it enhances the overall processing speed for concurrent operations.

As a result of these optimizations, we have successfully increased the sampling rate of the radar classification algorithm, leading to a significant improvement in its processing capabilities.

7. FUTURE WORK

In future research, the main focus could be on integrating a TOA-based deinterleaving algorithm and implementing a specialized database query system for threat identification in a library context. This approach aims to improve the effectiveness of threat detection mechanisms in this operational domain. Additionally, the investigation would extend to exploring and addressing Pulse-on-Pulse phenomena, especially in radar-rich environments with high signal density. This strategic consideration would strengthen the system's robustness in scenarios where overlapping radar pulses present challenges to conventional signal processing methods.

REFERENCES

1. De Martino, A. (2018). *Introduction to Modern EW Systems*. (2. Edition). Artech House.

2. Wiley, R. (2006). *ELINT: The Interception and Analysis of Radar Signals*. (1. Edition). Artech House.

3. Mitola, J. (1995). The software radio architecture. *IEEE Communications Magazine*, 33(5), 26-38.

4. Bagheri, R., Mirzaei, A., Heidari, M.E., Chehrazi, S., Lee, M., Mikhemar, M., Tang, W.K., Abidi, A.A. (2006). Software-defined radio receiver: dream to reality. *IEEE Communications Magazine*, 44(8), 111-118.

5. Wyglinski, A. M., Orofino, D. P., Ettus, M. N., Rondeau, T. W. (2016). Revolutionizing software defined radio: case studies in hardware, software, and education. *IEEE Communications Magazine*, 54(1), 68-75.

6. Baldini, G., Sturman, T., Biswas, A. R., Leschhorn, R., Godor, G., Street, M. (2012). Security aspects in software defined radio and cognitive radio networks: A Survey and A Way Ahead. *IEEE Communications Surveys & Tutorials,* 14(2), 355-379.

7. Abidi, A. A. (2007). The Path to the software-defined radio receiver. *IEEE Journal of Solid-State Circuits*, 42(5), 954-966.

8. Pető, T. (2015, July). *Multichannel passive radar receiver platform*. 17th International Conference on Transparent Optical Networks (ICTON), Budapest.

9. Licursi de Mello, R. G., Rangel de Sousa, F. (2021). Non-analytical direction-finding method as a key step in pursuing low size, weight, costs, and computational power in the deinterleaving of radar pulses. *IET Radar, Sonar & Navigation*, 13(11), 1876-1882.

10. Licursi de Mello, R. G., Rangel de Sousa, F. (2018). Precise techniques to detect superimposed radar pulses on ESM systems. *IET Radar, Sonar & Navigation*, 12(7), 735-741.

11. Revillon, G., Mohammad-Djafari, A., Enderli, C. (2019). Radar emitters classification and clustering with a scale mixture of normal distributions. *IET Radar, Sonar & Navigation, 13*(1), 128-138.

12. Licursi de Mello, R. G., Rangel de Sousa, F., Junqueira, C. (2017, August). *SDR-based radar detectors embedded on tablet devices*. SBMO/IEEE MTT-S International Microwave and Optoelectronics Conference (IMOC), Aguas de Lindoia.

13. Öncü, S., Kara, A. (2023). A mini-review on SDR based radar classification system: recent advances and challenges. *Journal of Science, Technology and Engineering Research*, 4(2), 124-129.

14. Skolnik, M. I. (1990). *Radar Handbook.* (2. Edition). McGraw Hill.

15. Adamy, D. (2001). *EW 101: A First Course in Electronic Warfare.* (1. Edition). Artech House.

16. Tsui, J. (2005). *Microwave receivers with electronic warfare applications*. (Reprint Edition). Scitech Publishing.

17. Lind, E., Stahre, M. (2020). *Deinterleaving of radar pulses with batch processing to utilize parallelism.* Doctoral dissertation, KTH School of Electrical Engineering and Computer Science, Stockholm.

18. Mardia, H. K. (1988, April). *Adaptive multidimensional clustering for ESM*. IEE Colloquium on Signal Processing for ESM Systems, London.

19. Alhashimi, A., Abdullah, S. N. (2007). Deinterleaving of radar signals and PRF identification algorithms. *IET Radar, Sonar & Navigation*, 1(4), 340-347.

20. Adamy, D. (2002). *Introduction to Electronic Warfare Modeling and Simulation*. (1. Edition). Artech House.

21. Sharma, P., Sarma, K. K., Mastorakis, N. E. (2020). Artificial intelligence aided electronic warfare systems: recent trends and evolving applications. *IEEE Access*, 8, 224761-224780.

22. Cheng, W., Zhang, Q., Dong, J., Wang, C., Liu, X., Fang, G. (2021). An enhanced algorithm for deinterleaving mixed radar signals. *IEEE Transactions on Aerospace and Electronic Systems*, 57(6), 3927-3940.

23. Li, X., Liu, Z., Huang, Z., Liu, W. (2020). Radar emitter classification with attention-based multi-RNNs. *IEEE Communications Letters*, 24(9), 2000-2004.

24. Machado, R. G., Wyglinski, A. M. (2015). Software-defined radio: Bridging the analog–digital divide. *Proceedings of the IEEE*, 103(3), 409-423.

25. Wyglinski, A., Pu, D. (2013). *Digital Communication Systems Engineering with Software-Defined Radio.* (1. Edition). Artech House.

26. Prager, S., Thrivikraman, T., Haynes, M., Stang, J., Hawkins, D., Moghaddam, M. (2018, April). *Ultra-wideband synthesis for high-range resolution software defined radar*. IEEE Radar Conference, Oklahoma City.

27. Molla, D. M., Badis, H., George, L., Berbineau, M. (2022). Software defined radio platforms for wireless technologies. *IEEE Access*, 10, 26203-26229.

28. Grimm, M., Allén, M., Marttila, J., Valkama, M., Thomä, R. (2014). Joint Mitigation of Nonlinear RF and Baseband Distortions in Wideband Direct-Conversion Receivers. *IEEE Transactions on Microwave Theory and Techniques*, 62(1), 166-182.

29. Kumar, N., Rawat, M., Rawat, K. (2020). Software-Defined Radio Transceiver Design Using FPGA-Based System-on-Chip Embedded Platform With Adaptive Digital Predistortion. *IEEE Access*, 8, 214882-214893.

30. Anttila, L., Lampu, V., Hassani, S. A., Campo, P. P., Korpi, D., Turunen, M., Pollin, S., Valkama, M. (2021). Full-Duplexing With SDR Devices: Algorithms, FPGA Implementation, and Real-Time Results. *IEEE Transactions on Wireless Communications*, 20(4), 2205-2220.

31. Schilcher, T. (2008). RF applications in digital signal processing. *CERN Accelerator School: Digital Signal Processing*, 249-283.

32. Mahafza, B. R. (2013). *Radar Systems Analysis and Design Using MATLAB*. (3. Edition). Chapman and Hall/CRC.

33. Robertson, S. (2019). *Practical ESM Analysis.* Artech House.

34. Ortatatlı, İ. E., Orduyılmaz, A., Serin, M., Özdil, Ö., Yıldırım, A., Gürbüz, A. C. (2016). *Real-time frequency parameter extraction for electronic support systems*. 24th Signal Processing and Communication Application Conference (SIU), Zonguldak.

35. Li, W., Tang, C., Vishwakarma, S., Woodbridge, K., Chetty, K. (2022). Design of high-speed software defined radar with GPU accelerator. *IET Radar, Sonar & Navigation*, 16(7), 1083-1094.

36. Wu, Z., Shi, L., Li, J., Wang, Q., Sun, L., Wei, Z., Plaza, J., Plaza, A. (2018). GPU Parallel Implementation of Spatially Adaptive Hyperspectral Image Classification. *IEEE Journal of Selected Topics in Applied Earth Observations and Remote Sensing*, 11(4), 1131-1143.

37. Internet: NVIDIA, (2024). *Fast Fourier Transform for NVIDIA GPUs*, Web: https://developer.nvidia.com/cuFFT, Last Access Date: 01.01.2024.

38. Adámek, K., Novotný, J., Thiyagalingam, J., Armour, W. (2021). Efficiency Near the Edge: Increasing the Energy Efficiency of FFTs on GPUs for Real-Time Edge Computing. *IEEE Access*, 9, 18167-18182.

39. Allevato, G., Hinrichs, J., Rutsch, M., Adler, J. P., Jäger, A., Pesavento, M., Kupnik, M. (2021). Real-Time 3-D Imaging Using an Air-Coupled Ultrasonic Phased-Array. *IEEE Transactions on Ultrasonics, Ferroelectrics, and Frequency Control*, 68(3), 796-806.

40. Pirgov, P., Mullin, L. and Khan, R. (2021). *Out-of-GPU FFT: A case study in GPU prefetching*. International Conference on Computational Science and Computational Intelligence (CSCI), Las Vegas.

41. Internet: FFTW, (2024). *Fastest Fourier Transform in the West*, Web: http://www.fftw.org, Last Access Date: 01.01.2024.

42. Ester, M., Kriegel, H.-P., Sander, J., Xu, X. (1996, August). *A density-based algorithm for discovering clusters in large spatial databases with noise*. Proceedings of the Second International Conference on Knowledge Discovery and Data Mining, Oregon, 226-231.

43. Chen, Y., Zhou, L., Pei, S., Yu, Z., Chen, Y., Liu, X., Du, J. and Xiong, N. (2021). KNN-Block DBSCAN: Fast Clustering for Large-Scale Data. *IEEE Transactions on Systems, Man, and Cybernetics: Systems*, 51(6), 3939-3953.

44. Li, S.-S. (2020). An Improved DBSCAN Algorithm Based on the Neighbor Similarity and Fast Nearest Neighbor Query. *IEEE Access*, 8, 47468-47476.

45. Gan, G., Ma, C., Wu, J. (2007). *Data Clustering: Theory, Algorithms, and Applications.* (1. Edition). Society for Industrial and Applied Mathematics.

46. Chandra, V., Jyotishi, B. K., Bajpai, R. C. (1988). *Some new algorithms for ESM data processing*. 20th Southeastern Symposium on System Theory, Charlotte, 108-112.

47. Dadgarnia, A., Sadeghi, M. T. (2023). A novel method of deinterleaving radar pulse sequences based on a modified DBSCAN algorithm. *China Communications*, 20(2), 198-215.

48. Internet: Ettus Research, (2024). *Ettus N320 SDR*. Web: https://www.ettus.com/all-products/usrp-n320/., Last Access Date: 01.01.2024.



Gazili olmak ayrıcalıktır